Version 2024-02-21

Supplementary Information

Recent reductions in aerosol emissions have increased Earth's energy imbalance

Øivind Hodnebrog[1], Gunnar Myhre[1], Caroline Jouan[1], Timothy Andrews[2], Piers M. Forster[3], Hailing Jia[4,a], Norman G. Loeb[5], Dirk J. L. Olivié[6], David Paynter[7], Johannes Quaas[4], Shiv Priyam Raghuraman[8], and Michael Schulz[6]

[1]Center for International Climate Research (CICERO), Oslo, Norway

[2]Met Office Hadley Centre, Exeter, UK

[3]Priestley Centre for Climate Futures, University of Leeds, Leeds, UK

[4]Institute for Meteorology, Leipzig University, Leipzig, Germany

[5]NASA Langley Research Center, Hampton, USA

[6]Norwegian Meteorological Institute, Oslo, Norway

[7]NOAA Geophysical Fluid Dynamics Laboratory, Princeton, NJ, USA

[8]Rosenstiel School of Marine, Atmospheric, and Earth Science, University of Miami, Coral Gables, FL, USA

[a]now at: SRON Netherlands Institute for Space Research, Leiden, Netherlands

Corresponding author: Øivind Hodnebrog (oivind.hodnebrog@cicero.oslo.no)

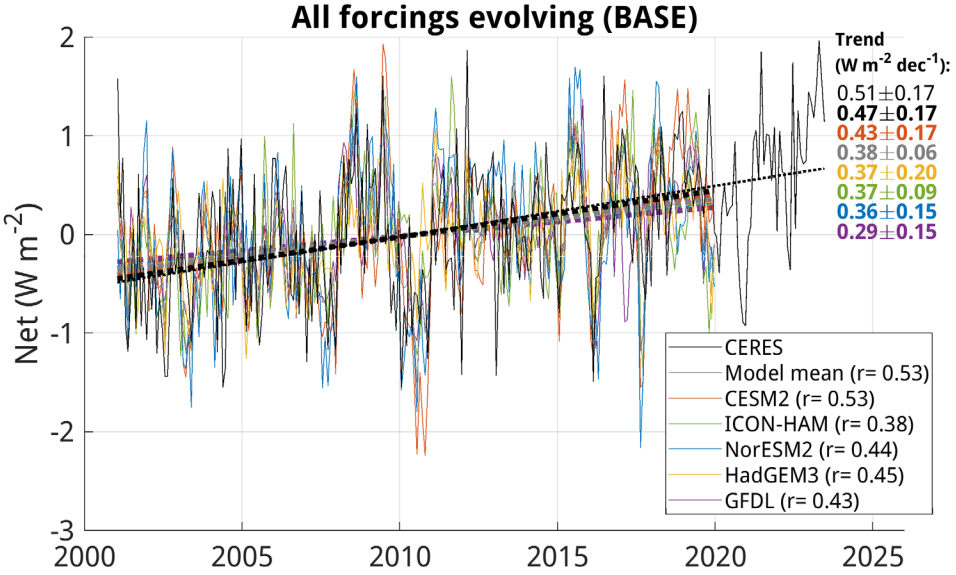

Supplementary Figure 1. Same as in Figure 1a in the main manuscript except that deseasonalized monthly values (ensemble mean for each model) rather than yearly values are shown. The black thin dotted line shows the CERES trend for January 2001 – June 2023 while the thick dotted lines show the January 2001 – December 2019 trends.

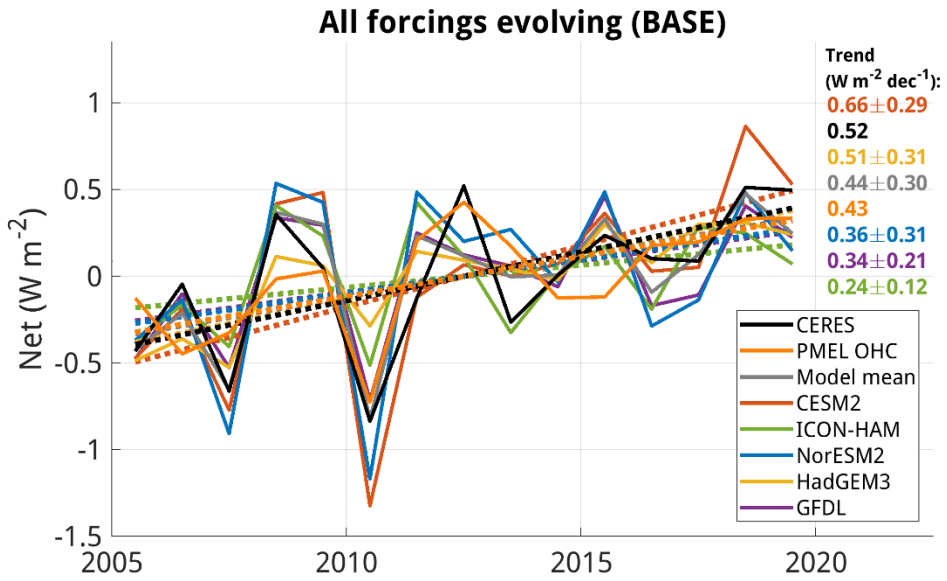

Supplementary Figure 2. Same as Figure 1a in the main manuscript except that annual ocean heat content (OHC) data from the Pacific Marine Environmental Laboratory (PMEL)[1] have been added as anomalies (thick solid orange line) and trend (thick dashed orange line), and that data are only shown for 2005-2019 and without individual ensemble members for the models.

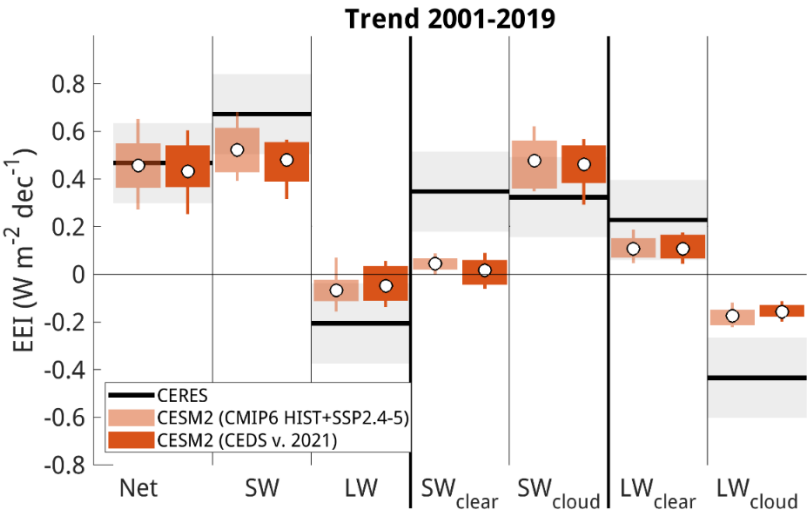

Supplementary Figure 3. Comparison of the global mean deseasonalized monthly 2001-2019 trend in top-of-atmosphere net, shortwave (SW) and longwave (LW) downward radiative flux between CERES and the CESM2 model run with both CMIP6 emissions (assuming SSP2-4.5 from 2015 onwards) and the newer (version April 2021) CEDS aerosol emission inventory that goes until 2019. SW and LW trends are shown separately for all-sky, clear-sky and the cloud radiative effect. Boxes represent the 90% and 66% confidence intervals and white dots show the mean of individual ensemble member trends. Grey shading shows the 5-95% confidence interval for CERES.

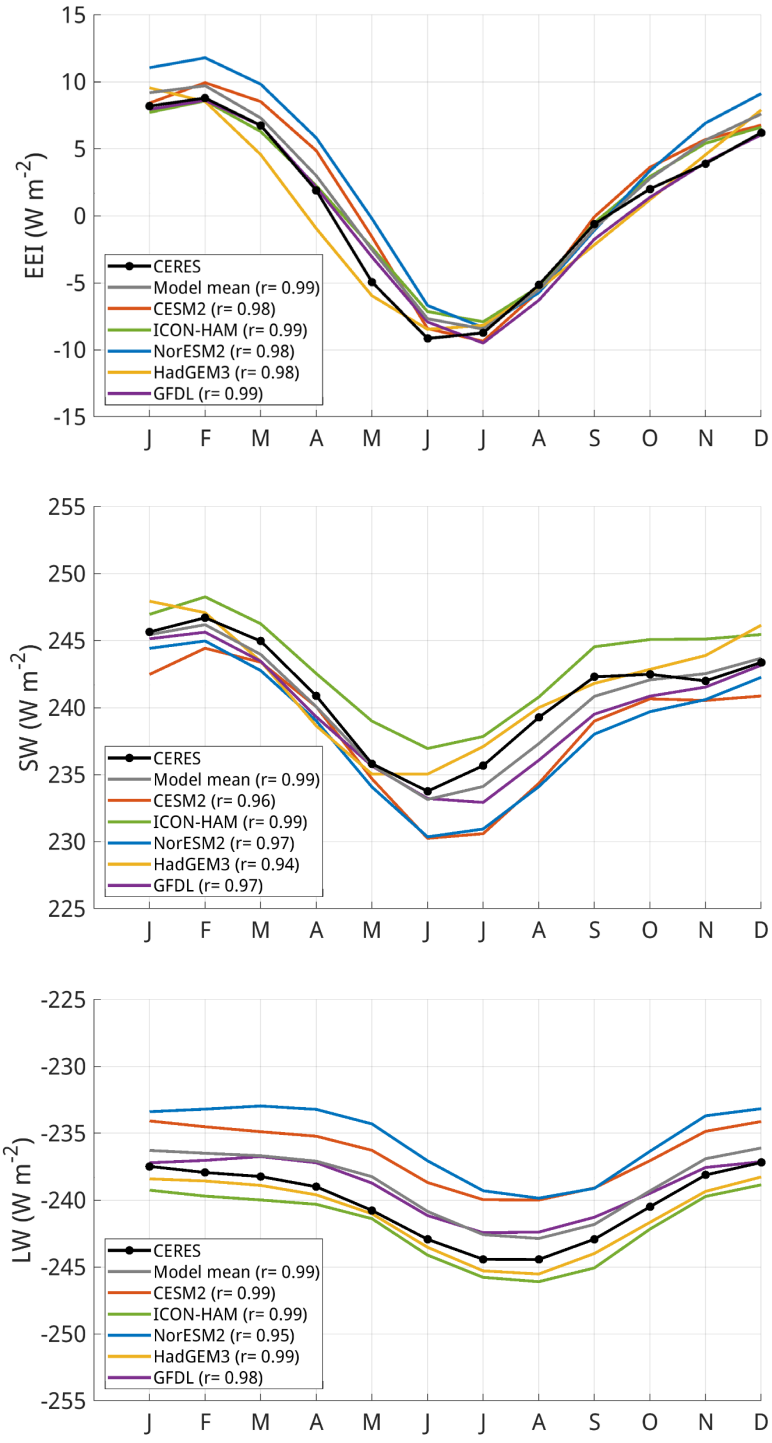

Supplementary Figure 4. Evaluation of the seasonal cycle of net (EEI; top), shortwave (SW; middle) and longwave (LW; bottom) fluxes at the top-of-atmosphere in each of the models' BASE experiment (mean of ensemble members) against CERES observations for the period 2001-2019. «Model mean» is the average of CESM2, ICON-HAM, NorESM2 and HadGEM3. Correlation coefficients (*r*) between CERES and models are shown in the legend.

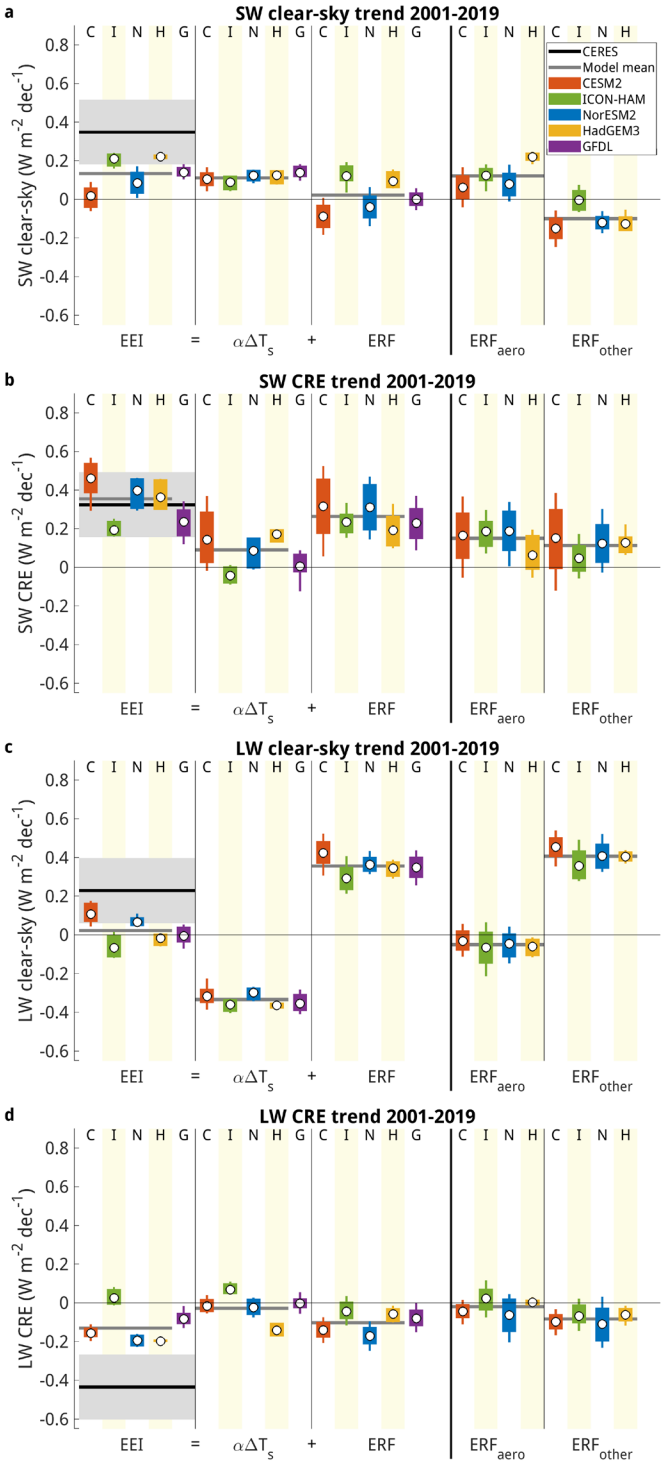

Supplementary Figure 5. Same as Figure 2 in the main manuscript except for **a** SW clear-sky, **b** SW cloud radiative effect (CRE), **c** LW clear-sky, and **d** LW CRE.

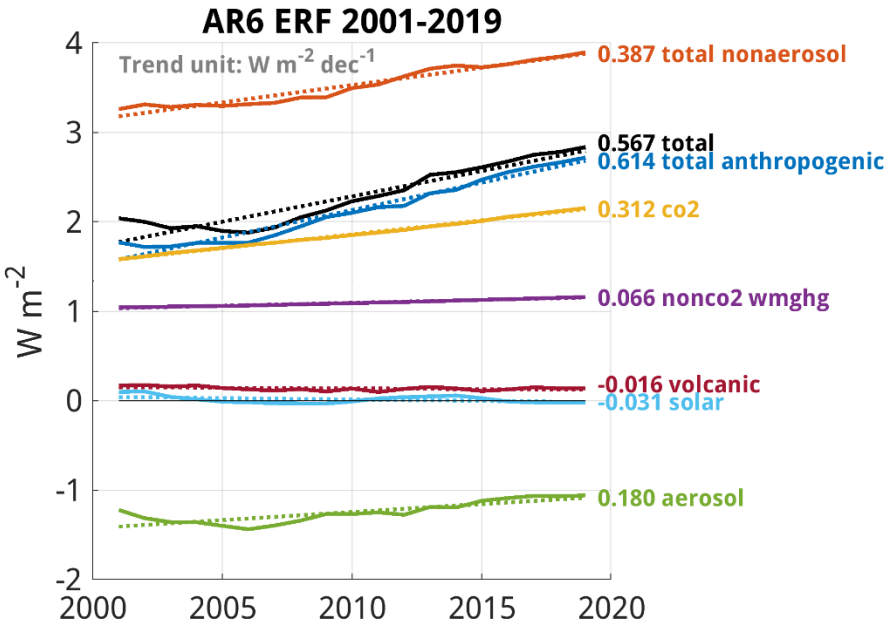

Supplementary Figure 6. Timeseries of effective radiative forcing (ERF) and their trend over the 2001-2019 period given for different anthropogenic and natural forcings, from the Intergovernmental Panel on Climate Change (IPCC) Assessment Report 6 (AR6)[2].

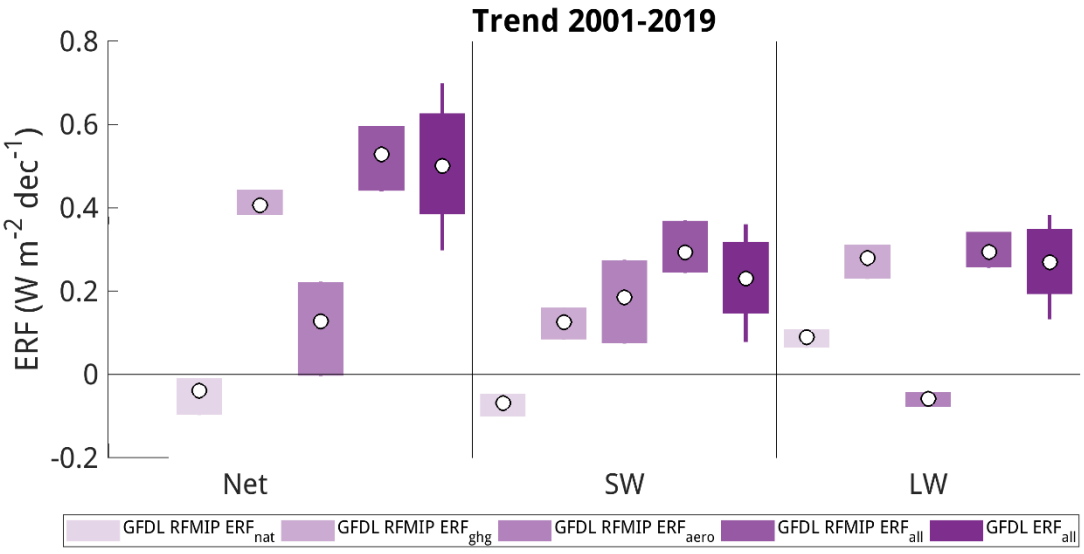

Supplementary Figure 7. Comparison of the global mean deseasonalized monthly 2001-2019 trend in top-of-atmosphere net, shortwave (SW) and longwave (LW) downward radiative fluxes between GFDL simulations within RFMIP[3]. The different bars show the trend due to natural forcings (ERF_{nat}; experiment piClim-histnat), greenhouse gas forcing (ERF_{ghg}; piClim-histghg), aerosol forcing (ERF_{aero}; piClim-histaer), and all forcings (ERF_{all}; piClim-histall). ERF_{all} is shown both for the RFMIP simulations and the "AM4 PSST ERF" minus "AM4 PSST" (equivalent to BASE-ALL2000) simulations. Boxes represent the 90% and 66% confidence intervals and white dots show the mean of individual ensemble member trends (3 ensemble members for RFMIP and 20 members for BASE and ALL2000).

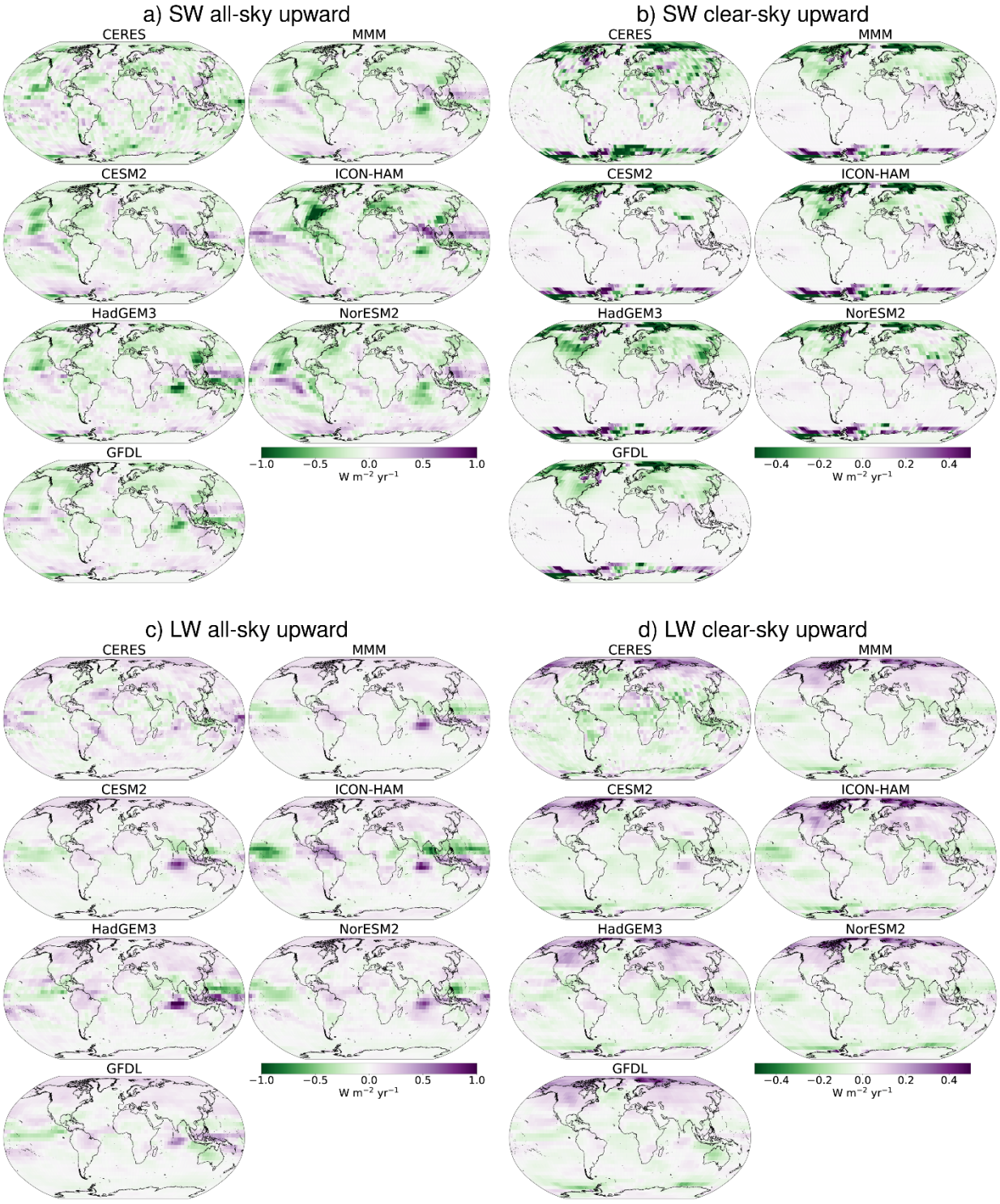

Supplementary Figure 8. Comparison of the 2001-2019 trends between models and CERES **a** SW all-sky, **b** SW clear-sky, **c** LW all-sky, **d** LW clear-sky, **e** net all-sky and **f** net clear-sky, and MODIS **g** aerosol optical depth, **h** total cloud fraction and **i** liquid water path. Note that trends in SW and LW radiative fluxes (**a**-**d**) show upward radiation, and therefore have positive values when more radiation is sent back to space, while net radiation fluxes are positive downward.

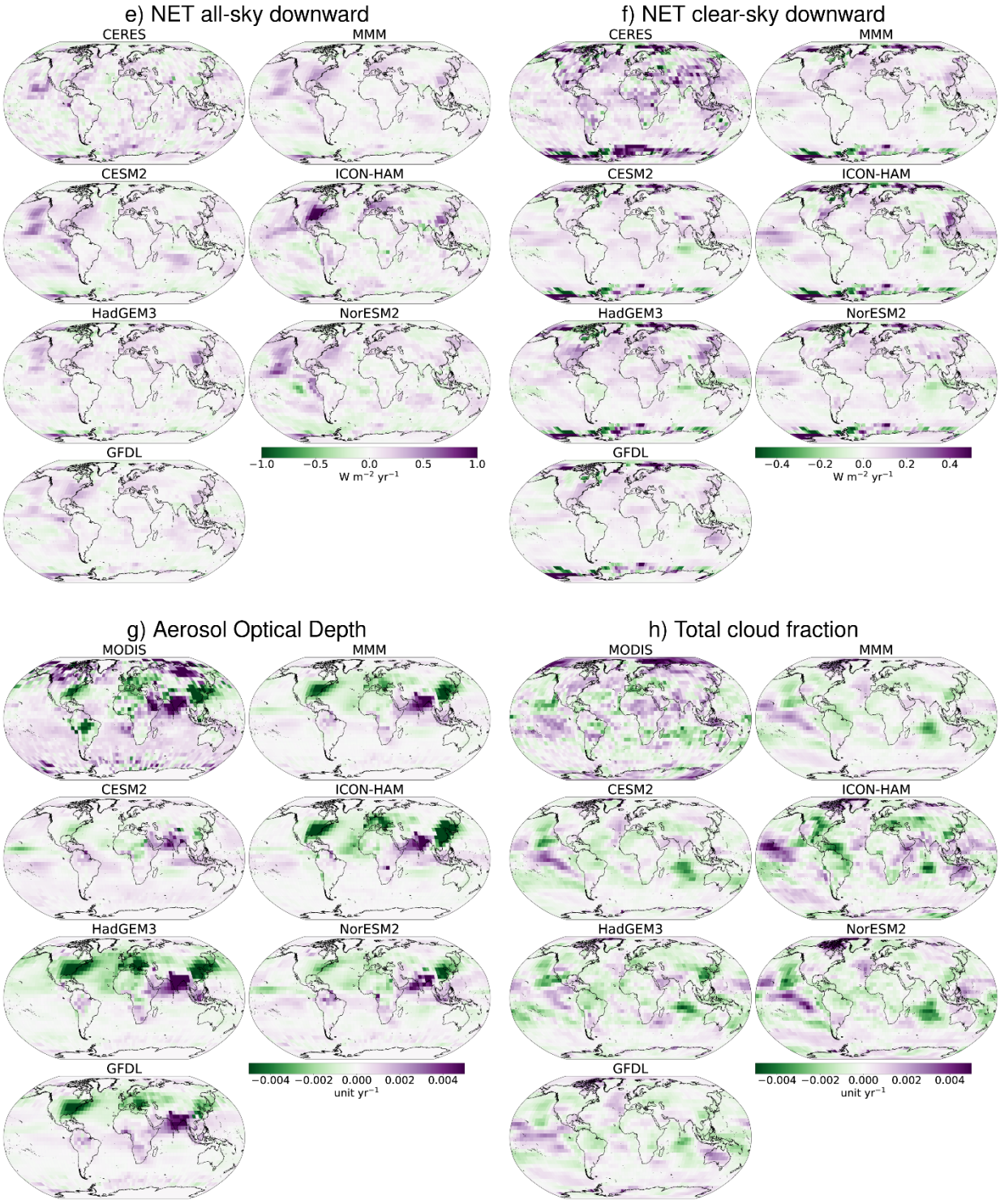

Supplementary Figure 8 cont.

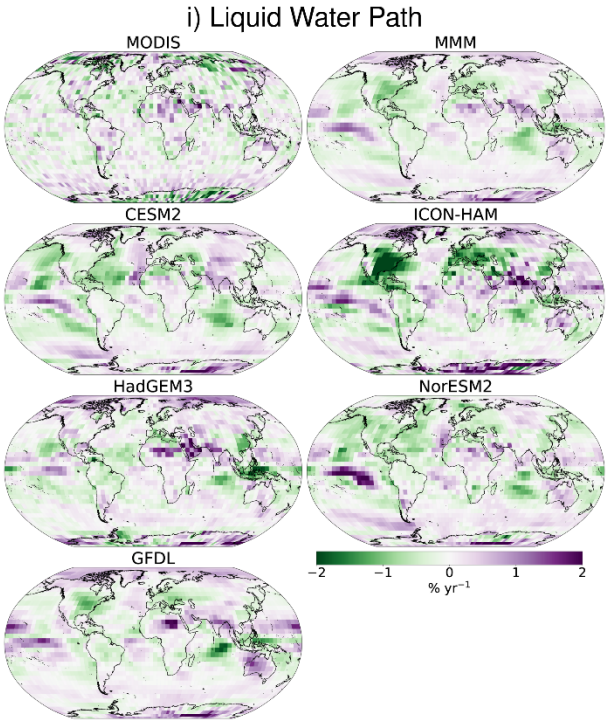

Supplementary Figure 8 cont.

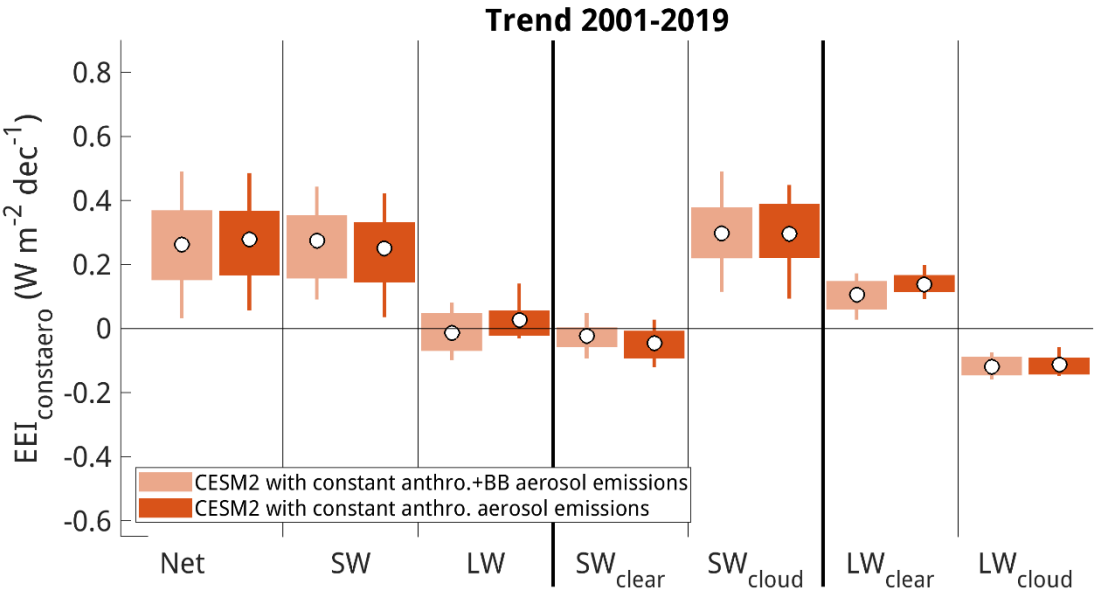

Supplementary Figure 9. Comparison of the global mean deseasonalized monthly 2001-2019 trend in top-of-atmosphere net, shortwave (SW) and longwave (LW) downward radiative fluxes between a CESM2 simulation where both anthropogenic and biomass burning aerosol emissions have been kept constant and one where only anthropogenic aerosol emissions have been kept constant. SW and LW trends are shown separately for all-sky, clear-sky and the cloud radiative effect. Boxes represent the 90% and 66% confidence intervals and white dots show the mean of individual ensemble member trends.

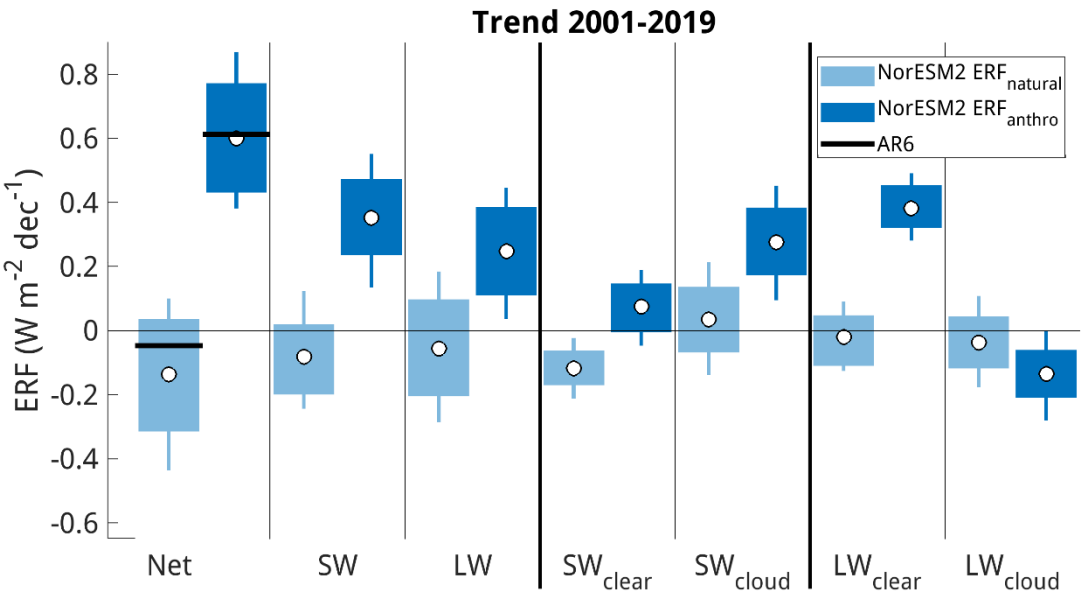

Supplementary Figure 10. Comparison of the global mean deseasonalized monthly 2001-2019 trend in top-of-atmosphere net, shortwave (SW) and longwave (LW) downward radiative flux differences between NorESM2 simulations ANTHRO2000-ALL2000, showing the trend due to natural forcings ($ERF_{natural}$), and BASE-ANTHRO2000, showing the trend due to anthropogenic forcings (ERF_{anthro}). SW and LW trends are shown separately for all-sky, clear-sky and the cloud radiative effect. Boxes represent the 90% and 66% confidence intervals and white dots show the mean of individual ensemble member trends.

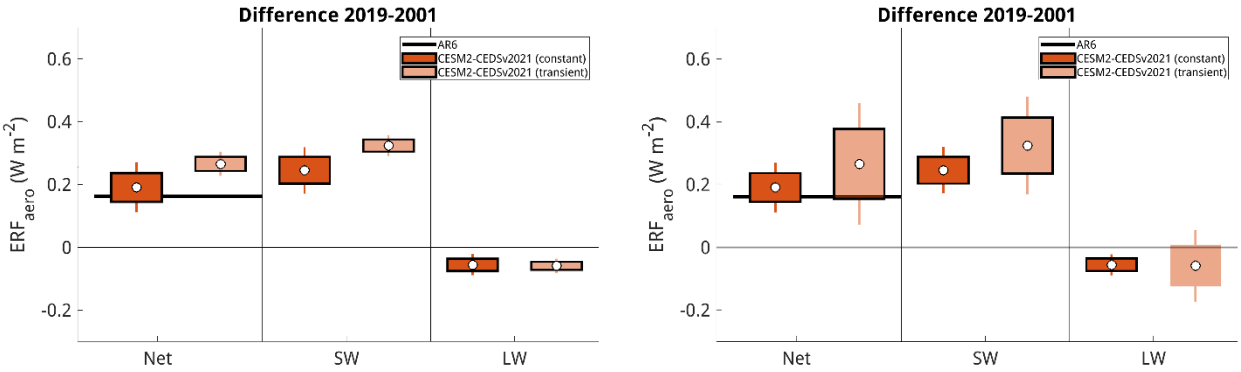

Supplementary Figure 11. Box plot showing the 90% and 66% confidence intervals of the difference 2019-2001 in the ERF of anthropogenic aerosols from separate experiments using 2000 climatology ("constant") compared with the difference BASE-AERO2000 ("transient"), split into net, SW all-sky and LW all-sky. In the left plot, all possible combinations of ensemble members were used for the BASE minus AERO2000 difference, while in the right plot, box plots were based on BASEn01 minus AERO2000n01, BASEn02 minus AERO2000n02, ..., BASEn20 minus AERO2000n20. Black rectangles indicate that differences between simulations are statistically significant ($p<0.05$) based on a two sample *t*-test.

Supplementary References

1 Loeb, N. G. *et al.* Satellite and Ocean Data Reveal Marked Increase in Earth's Heating Rate. *Geophys. Res. Lett.* **48**, doi:10.1029/2021gl093047 (2021).

2 Forster, P. M. *et al.* in *Climate Change 2021: The Physical Science Basis. Contribution of Working Group I to the Sixth Assessment Report of the Intergovernmental Panel on Climate Change* (eds V. Masson-Delmotte *et al.*) Ch. 7, (Cambridge University Press, 2021).

3 Raghuraman, S. P., Paynter, D. & Ramaswamy, V. Anthropogenic forcing and response yield observed positive trend in Earth's energy imbalance. *Nature Communications* **12**, doi:10.1038/s41467-021-24544-4 (2021).